APPLIED BIOCHEMISTRY AND BIOTECHNOLOGY 9, 27–39 (1984)

Diffusion and Reaction in an Immobilized-Enzyme Starch Saccharification Catalyst

D. A. SIROTTI*,† AND A. H. EMERY

School of Chemical Engineering, Purdue University, West Lafayette, IN 47907

Received June 17, 1983; Accepted September 20, 1983

Abstract

Effectiveness factors were predicted from measurements of basic parameters made on single oligosaccharides, and the prediction was compared to experimental effectiveness factors for the reaction of each oligosaccharide in the immobilized enzyme catalyst. Kinetic parameters were obtained for the hydrolysis of each oligosaccharide catalyzed by soluble glucoamylase, and were fit with a subsite model equation capable of generalization to all sizes of oligosaccharide. Diffusion coefficients in free solution were determined from movement out of a capillary tube. Spatial characteristics of the immobilized enzyme bed were obtained from pulse response experiments, allowing the calculation of effective diffusivities. Experimental effectiveness factors plotted against modulus were in reasonable agreement with the predictions.

Index Entries: Diffusion, in an immobilized enzyme catalyst; reactions, in an immobilized enzyme catalyst; immobilized-enzyme, starch saccharification catalyst; enzyme, immobilized, as a starch saccharification catalyst; starch saccharification catalyst, immobilized enzyme; saccharification catalyst, starch; catalyst, starch saccharification.

Introduction

The interplay between diffusion and reaction is especially interesting during the reactions that produce glucose from starch hydrolyzates in an immobilized enzyme

*Author to whom all correspondence and reprint requests should be addressed.

†Present address: The Upjohn Company, Kalamazoo, MI 49001

0273-2289/84/0200-0027$02.60

catalyst particle. There occurs not a single reaction but a series of sequential reactions that remove one glucose unit at a time from each oligosaccharide. As the molecules become shorter, both the reaction rate and the diffusion rate change. The longer dextrins have higher reaction rates at a given concentration. In the Michaelis-Menten model, they would have a larger V_{max} and a smaller K_M. In addition, because they are larger molecules they have lower diffusivities. These conditions tend to give higher values for the Thiele modulus, causing situations where diffusional limitations are relatively more severe. The shorter dextrins are slower reacting and faster diffusing, thereby giving smaller modulus values and situations where diffusional limitations are less severe. As the reaction proceeds towards full conversion to glucose, the longer dextrins are successively converted to shorter ones, changing the relative diffusion and reaction rates.

The work described here involves the study of the reactions of several individual purified maltodextrins with both soluble and immobilized glucoamylase enzyme. The work encompasses the determination of kinetic parameters for the pure reactants and soluble enzyme, the determination of diffusion coefficients of the pure reactants, the determination of effectiveness factors for certain reaction conditions with the immobilized enzyme, and the associated theoretical analyses of the reaction and diffusion phenomena. If the enzyme kinetics do not change upon immobilization, a usual effectiveness factor analysis based on the soluble enzyme kinetic parameters should predict the immobilized catalyst performance.

Published work by Swanson et al. (*1*) showed that the experimental effectiveness factors for reactions at different conditions of particle radius, activity, and maltose concentration followed the expected dependence on the calculated general modulus. That study involved a single reactant, maltose, and covered a range of effectiveness factors from unity down to under 10%. Recently published work by Lee et al. (*2*) showed that the concentration profiles for groups of components during the reaction of a commercial dextrin mixture were different with larger glass beads than with smaller beads or with the soluble enzyme, definitely a result of diffusional limitations. Because the larger reactants reacted faster and diffused more slowly, the concentration profiles for a set of reaction conditions depended on the extent of diffusional limitations.

Reaction Modeling

Two approaches can be taken to model the kinetics of the enzyme reactions. The first is to model each reactant separately using Michaelis-Menten expressions; each reactant i would then have the two associated parameters $V_{max,\,i}$ and $K_{M,\,i}$. The total number of parameters would be twice the number of reactants being modeled. More parameters would be needed if, for example, substrate inhibition were important.

The second approach recognizes that there must be something mechanistically similar among the various maltodextrin reactions, since all are catalyzed by the same active site. A subsite model has been proposed in past studies (*3*) as a model for depolymerase enzymes such as glucoamylase. The model assumes that each

glucose unit of the maltodextrin interacts in some way with the enzyme "surface," and that these interactions can be visualized in terms of binding at discrete subsites. The parameters for the model include a binding energy for each subsite, plus one rate constant for the hydrolysis of a properly-attached molecule. The single rate constant is assumed to be independent of the chain length of the attached molecule. By allowing "higher-order" binding modes, such as the nonproductive complex shown in Fig. 1, severe departures from Michaelis-Menten kinetics that occurred with high maltose concentrations could be predicted (*4*). The advantage of the subsite model is that it is mechanistically fundamental yet also potentially requires fewer parameters than the series of Michaelis-Menten equations.

Materials and Methods

Sugar Assays

Total carbohydrates were measured by an orcinol–sulfuric acid assay (*5*). Samples containing alcohols, such as the *t*-butanol used to elute the carbon column, were evaporated to dryness before assay to prevent interference with the color development. The Somogyi-Nelson reducing copper assay (*6*, *7*) was used to measure molar concentrations of the maltodextrins. Unlike the dinitrosalicylic acid (DNS) method, the Somogyi-Nelson assay gives a constant molar absorbancy for the homologous series of maltodextrins, independent of chain length.

End groups of the maltodextrin chains were analyzed by a periodic acid reaction (*8*), which oxidizes vicinal carbons having hydroxyl groups to aldehydes. When three such carbons exist together, the central one is liberated as formic acid. Each nonreducing end group of a maltooligosaccharide thus releases one formic acid molecule, each reducing end releases two, while interior glucose moieties release none. This data, coupled with the results of the Somogyi-Nelson assay, yield information about the number of branches per chain.

The Beckman glucose analyzer was used to measure glucose concentrations above about 0.1 mg/mL. To prevent interference from high maltodextrin concentrations, caused by small amounts of maltase and amylase activities in the

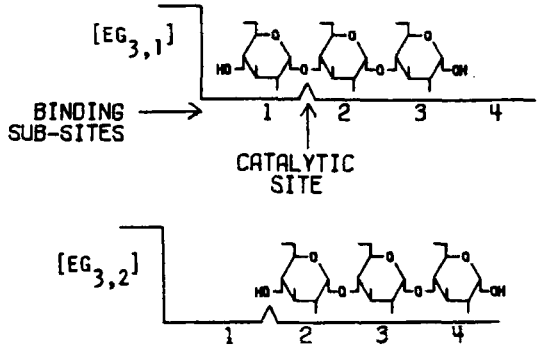

Fig. 1. Schematic representations of maltotriose bound to glucoamylase in "productive" complex ($EG_{3,1}$) and "nonproductive" complex ($EG_{3,2}$).

Beckman glucose oxidase reagent, the reagent was diluted with one-half volume of 1.0*M* tris(hydroxymethyl)aminomethane hydrochloride buffer at pH 5.7, which inhibits carbohydrase activities (*9*).

A kinetic glucose assay was used to measure lower concentrations of glucose. The assay reagent consisted of 0.2 mL of 1560 U/mL glucose oxidase solution (Sigma Chemical G-6500, a preparation free of carbohydrases), 2.5 mg peroxidase (Sigma P-8250), 25 mL of pH 5.3 buffer containing 0.23*M* Tris and 0.36*M* NaH_2PO_4, and 1.0 mL of 6.6 mg/mL *o*-dianisidine hydrochloride (Sigma). A cuvet containing 2.2 mL of this reagent was placed in a 25°C controlled-temperature cell holder in a Coleman Model 124 spectrophotometer. The absorbance at 463 nm was recorded on a strip-chart recorder. After a baseline was achieved a 0.1 mL sample containing no more than 5 μg glucose was added and mixed quickly. The initial slope of the absorbance response was correlated with glucose standards to calibrate the assay.

Protein Assays

Protein concentrations were measured approximately by the absorbance at 280 nm, or more accurately with the Bio-Rad protein assay kit (500-0001) calibrated with a bovine gamma-globulin standard.

Reactant Preparation

The chromatography column used to purify the maltodextrins was fashioned according to the procedures of Whelan (*10*) and French (*11*). The packing, consisting of 750 g powdered carbon (Darco G-60, Atlas Powder Company) and 600 g filter aid (Celite 560, Johns-Manville) was stirred in 6 L of 1*N* HCl overnight and rinsed with water. The acid-washed material was then stirred in 5.6 L of 2.5% stearic acid in ethanol for 2 h, washed with 2.5 L of 95% ethanol, then 1 L of 50% ethanol, and then dried overnight at 95°C. The solids were reslurried in water and packed into a 6.5-cm diameter glass column to give a bed 85 cm deep.

A solution of maltodextrins from partially hydrolyzed corn starch (Maltrin M-100, Grain Processing Company) was fractionated by adding four volumes 95% ethanol to precipitate the undesired higher molecular weight components. The supernatant was dried to remove the alcohol. The carbon column was loaded with about 5 g of the solids as a 15% solution in water, followed by a several liter water wash. The sugars were eluted with a step gradient of *t*-butanol in water, beginning at 1% concentration and increasing in 0.5% increments using 2–3 L at each step. Effluent fractions were assayed by the orcinol–sulfuric acid method, and pools were filtered, concentrated, and dried. A typical run is shown in Fig. 2. Unidentified minor impurities were removed by a contact with a mixed-bed ion exchange resin (Bio-Rad AG501-X8).

Analysis of each purified sugar by HPLC (*12*) showed a single clean peak. Results of the Somoygi-Nelson and periodate assays confirmed that the preparations were linear chains, with one equivalent of reducing ends and one equivalent of non-reducing ends per molar weight.

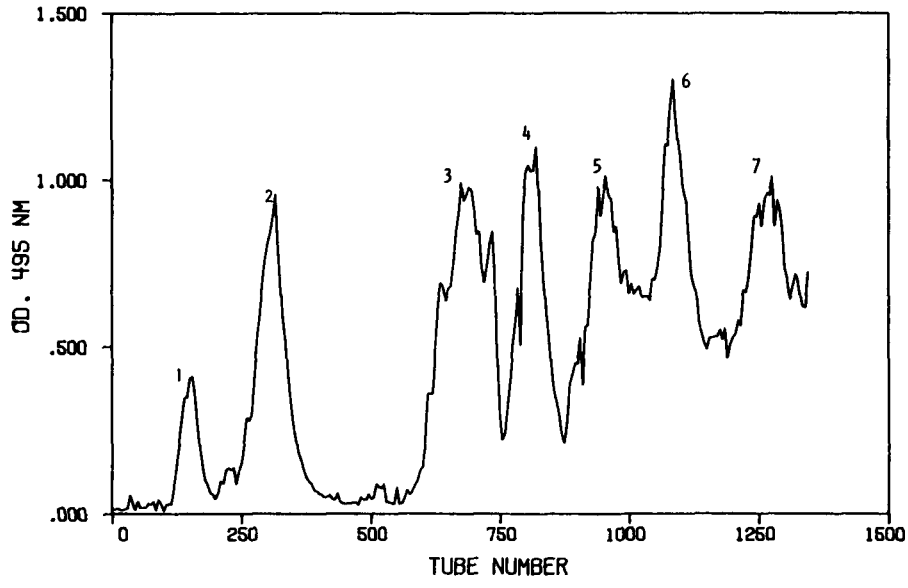

Fig. 2. Separation of maltodextrins via carbon column chromatography. Numbers denote chain lengths of eluted sugars.

Enzyme Preparation

Glucoamylase from *Aspergillus niger* (Diazyme 325 Lot F-5322-P, Miles Laboratories), in the form of a dry yellow powder, was slurried in water. The insolubles were centrifuged out and the brown supernate was vacuum-concentrated. The enzyme solution was further purified on a DEAE–cellulose column equilibrated with 0.1*M* citrate–phosphate buffer at pH 8.0, and eluted with a step gradient of the buffer at pH 8, 6, and 4. A typical run is shown in Fig. 3. Glucoamylase activity was detected only in the single large peak that began eluting at pH 5.8. The peak containing the activity was concentrated, dialyzed against distilled water, and further concentrated to give a colorless solution at 12 g/L protein and a specific activity of about 0.3 mol/s kg (measured with 0.8*M* maltose at pH 4.5, 50°C).

Enzyme Immobilization

The purified enzyme was immobilized onto controlled-pore ceramic beads (Corning Glass Works, 42.5 nm nominal pore diameter) via the silane–glutaraldehyde method of Brotherton et al. (*13*). Sufficient protein was used to load the activated support to capacity. The total reaction time for the enzyme binding reaction was 20 h. Figure 4 shows the effect of the amount of protein added on the amount bound (measured as the amount disappearing from solution). Added protein is completely bound until the maximum capacity is attained.

Diffusion Coefficients

Free-solution diffusivities were measured by a capillary diffusion technique (*14*). Small single-ended capillaries approximately 3 cm long and 0.18 cm diameter con-

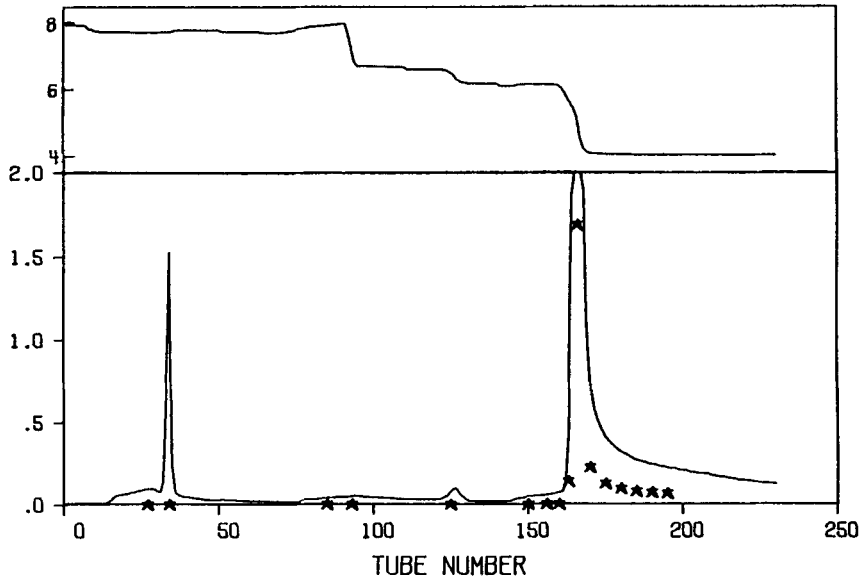

Fig. 3. Purification of glucoamylase via DEAE-cellulose chromatography. Stars represent relative activity measured with maltose hydrolysis.

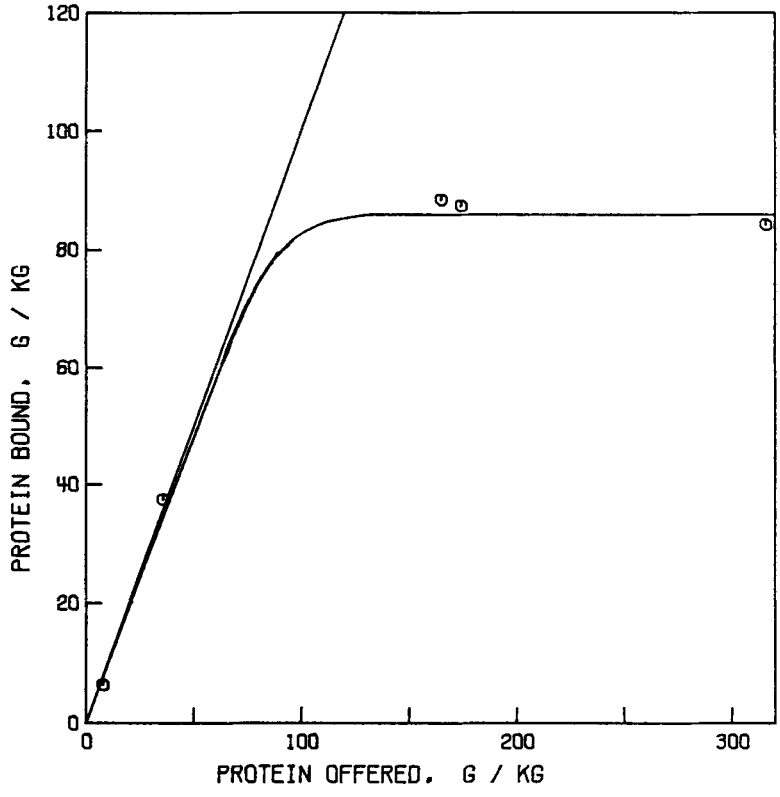

Fig. 4. Effect of amount of added protein on the amount bound during the immobilization reaction.

taining a solution of the sugar were immersed into a water reservoir. Tubes were withdrawn periodically and the amount of remaining sugar was measured. The experimental details are documented elsewhere (*15*).

The diffusion equation describing an analogous heat-transfer problem is solved in Carslaw and Jaeger (*16*). Assuming a constant diffusivity D, a uniform initial concentration C_o within the tube, and a constant zero external concentration, the result can be rewritten as:

$$c(x, t) = 4C_o/\pi \sum_{n=0}^{\infty} (-1)^n/(2n + 1) \cos[(2n + 1)\pi X/2L] \exp[-D(2n + 1)^2(t\pi^2/4L^2)] \quad (1)$$

where x is the distance from the closed end of a tube of length L. The average concentration over the length of the tube is:

$$\bar{c}(t)/C_o = 8/\pi^2 \sum_{n=0}^{\infty} 1/(2n + 1)^2 \exp[-D(2n + 1)^2 (t\pi^2/4L^2)] \quad (2)$$

Nonlinear regression of $\bar{c}(t)/c_o$ vs $t\pi^2/4L^2$ will give the diffusivity D.

Effective diffusion coefficients for the sugars within the ceramic pores were measured by the method of moment analyses of pulse responses (*17, 18*). Physical characteristics of a packed column of the immobilized enzyme catalyst were determined by first-moment analyses of large excluded molecules (500,000 mw dextran) and small molecules (glucose, cellobiose, ethylene glycol). An effective diffusivity for glucose was determined from second-moment analyses. From this a value for the tortuosity was obtained, which was then used to calculate effective diffusion coefficients for the longer chain dextrins. The experimental details are documented elsewhere (*15, 23*).

Soluble Enzyme Kinetics

Glucoamylase solution was added to tubes containing 50 m*M* acetate buffer pH 4.5 and varied concentrations of the maltodextrin at 50°C. Samples were withdrawn periodically for 30 min, and were quenched by placing immediately into either a tube containing one-tenth volume of 10% perchloric acid or a tube that had been in a boiling water bath for 3 min before sampling and 1 min afterwards. After a sufficient time for the mutarotation of the glucose product to equilibrate, the samples were assayed for glucose concentration. Conversions were held to under 10%, and reaction rates were determined from initial slopes.

Immobilized Enzyme Kinetics

The catalyst was packed into glass reactors 0.36 cm diameter by 4.6 cm length, through which 50°C sugar solutions buffered at pH 4.5 with 50 m*M* acetate were pumped at the desired flow rate and concentration. Glucose concentrations in the effluent were measured to determine conversion. Reactions with maltotetraose and maltohexaose were run using a fixed number of catalyst beads (265 ± 22 μm diameter) held in a basket reactor. The basket, formed of 100 mesh brass screen at-

tached to the top and bottom of an annular spacer, was agitated axially through a cylindrical vessel containing the reactant solution. Rate data were taken at sufficiently high column flow rates or basket agitation conditions that the reaction showed no further dependence on flow or agitation; film diffusion limitations were therefore insignificant.

Experimental Results

Soluble Enzyme Kinetics

The model developed by Swanson (*4*) to account for secondary binding modes at high maltose concentrations, Eq. (3), was used to correlate the rate data for the maltose reactions with the soluble enzyme:

$$V = V_{max} fS(1 + K_3S)/(K_M + S + fK_3S^2) \tag{3}$$

The maltotetraose and maltohexaose reaction data were correlated with the Michaelis-Menten model, Eq. (4). Concentrations of these substrates were never sufficiently large enough to exhibit the same deviations as the maltose data.

$$V = V_{max}S/K_M + S \tag{4}$$

The rate parameters determined by regression are listed in Table 1. The reaction parameters were analyzed (*15*) in terms of the subsite model (*3*) to give the results shown in Table 2.

The rate equations based on the subsite model are:

$$r_{G1} = k_oW \sum_{n=2}^{m} (K_{n,\,1}G_nE) + k_oWK_{2,\,1}G_2E \tag{5}$$

$$(n > 2)r_{G_n} = -k_oWK_{n,\,1}G_nE + k_oWK_{n+1,\,1}G_{n+1}E \tag{6}$$

where

$$E = E_T/[1 + \sum_{n=1}^{m} (K_{n,\,1} + K_{n,\,2})G_n] \tag{7}$$

TABLE 1
Physical and Rate Parameters

Parameter	Units	G2	G4	G6
D, (T °C)[a]	m^2/s	4.1×10^{-10}	3.8×10^{-10}	2.7×10^{-10}
D, (50 °C)[b]	m^2/s	8.3×10^{-10}	6.5×10^{-10}	4.8×10^{-10}
V_{max}	mol/s-kg	0.472	1.01	1.63
K_M	mol/m^3	1.75	0.70	0.23
f	—	0.55	—	—
K_3	m^3/mol	0.010	—	—

[a]Experimental diffusivity at 20°C (G2) and 25°C (G4, G6).
[b]Diffusivity corrected to 50°C, assuming constant D_μ/T.

TABLE 2
Determination of Subsite Model Parameters

	Binding constants for binding modes 1, 2, 3			
n, Reactant	$k_o K_{n,1}$	$k_o K_{n,2}$	$k_o K_{n,3}$	
2	0.149	0.116	0.0049	
3	0.322	—	—	(ref. *19*)
4	1.45	—	—	
6	7.09	—	—	

	Sum of binding energies, kJ/mol	
Subsite group	*A. niger*, this work	*R. delemar* (ref. *3*)
A1 + A2	15.3	20.2
A2 + A3	14.6	26.8
A3 + A4	6.1	8.5
A5 + A6	4.3	1.4
A1 + A2 + A3 + A4 + A5 + A6	25.7	30.0

The binding constants $K_{n,j}$ are calculated from the binding energies of the covered subsites by an equation given by Hiromi (*3*):

$$K_{n,j} = \exp(-10{,}000/RT)\exp\left(\sum_{i}^{\text{cov}} A_i/RT\right)_{n,j} \tag{8}$$

where the summation is taken for all occupied subsites, and the 10,000 J/mol arises from the mixing entropy in water.

Diffusivity Measurements

Results of the free-solution diffusion experiments described above are listed in Table 1. Figure 5 shows the data for maltotetraose plotted according to Eq. (2). The coefficients for maltotetraose and maltohexaose are within 12% of values predicted by a method of Othmer and Thakar (*20*).

The moment analyses of the pulse response tests gave an external void fraction ϵ of 0.44, an internal porosity β of 0.70, and a tortuosity τ of 1.6 (measured with glucose). These values of β and τ were used to calculate effective diffusivities of other species by

$$D_e = D(\beta/\tau) \tag{9}$$

Immobilized Enzyme Kinetics

Reaction rates measured in the immobilized enzyme reactors are listed in Table 3 with the reaction conditions. For each of the three catalyst preparations, the high-concentration maltose rates, assumed to be free of diffusional limitations, were used to determine the catalyst specific activity and to normalize the three sets of data. Subsequent calculations show the assumption valid, since modulus values were much below unity for those conditions. The normalized rates are shown in

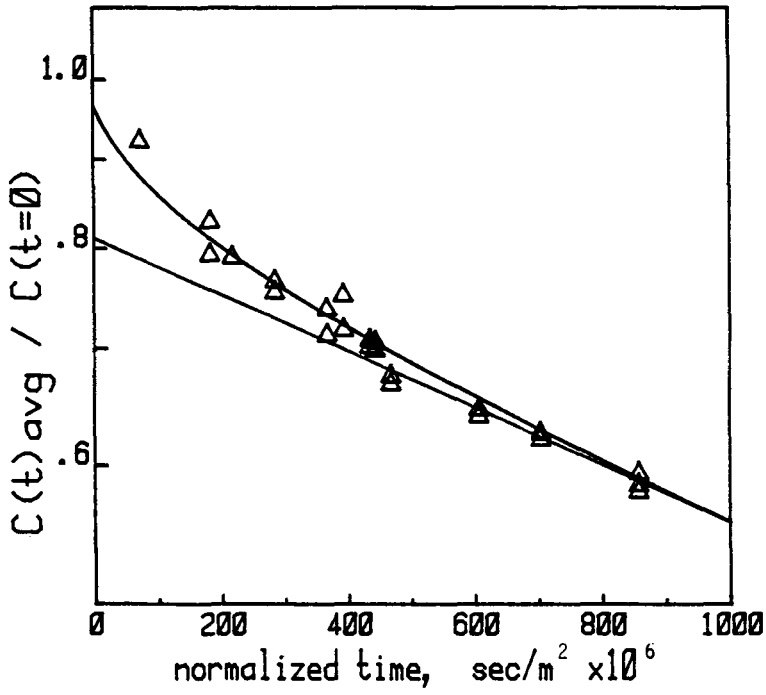

Fig. 5. Maltotetraose diffusion coefficient test results. Horizontal axis is normalized time, $t\pi^2/4L^2$. Curve is Eq. (2) result for best-fit value of D; straight line represents limiting slope.

Table 3 in terms of substrate reacted rather than glucose produced. In so doing, an assumption is made that subsequent reactions of the products contribute only insignificantly to the measured glucose production rate.

These reaction rates for the three reactants are plotted in Fig. 6 as functions of concentration superimposed on the three rate curves for the soluble enzyme. The extents to which the rates fall short of the soluble catalyst curves are taken to be effects of diffusional limitations at the lower concentrations. The ratios give the effectiveness factors η, which are listed in Table 3.

Calculation of Modulus

Inserting the Michaelis-Menten model, Eq. (4), into the generalized modified-Thiele modulus defined by Bischoff (*21*) and Aris (*22*), and performing the necessary integrations, gives the following expression for the reaction modulus:

$$\phi = [L\sqrt{k/(2K_M D_e)}] \times [(C_S/K_M)/(1 + C_S/K_M)\sqrt{1/(C_S/K_M - \ln(1 + C_S/K_M))}] \quad (10)$$

where L is the characteristic length of the particle, c_s is the surface concentration, and k corresponds to V_{max}. The first factor represents a first-order reaction modulus, and the second factor results from the effect of saturation where the kinetics approach zero-order as c_S/K_M approaches zero. The corresponding modulus for the maltose kinetics, more difficult to solve analytically, was evaluated numeric-

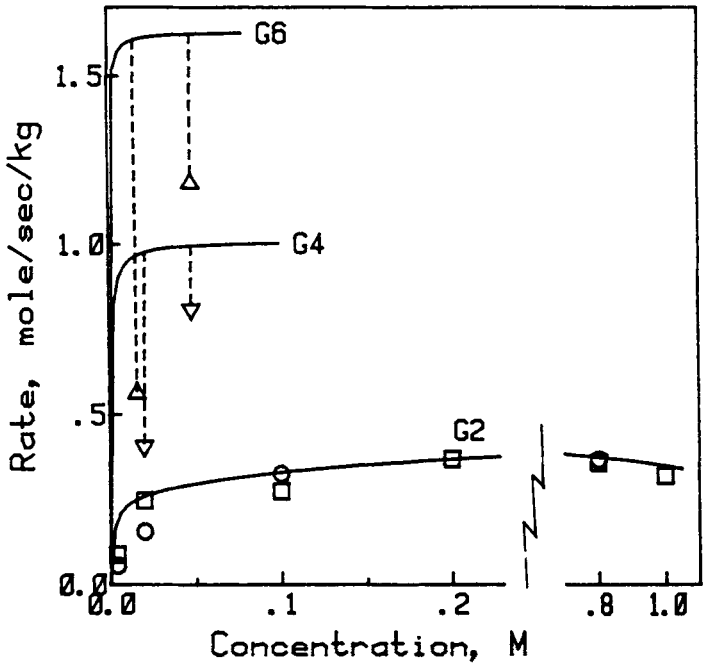

Fig. 6. Immobilized enzyme reaction rates. Curves represent calculated rates for the soluble enzyme.

TABLE 3
Immobilized Enzyme Reaction Results

Test	Catalyst activity[a]	Reactant	Conc., m*M*	Glucose production rate[b]	Normalized reaction rate[c]	*n*	ϕ
1	20.7	G2	1000	2.36	0.316	0.91	0.19
2			200	2.77	0.372	1.04	0.47
3		G4	48	2.98	0.797	0.81	1.70
4			20	1.51	0.404	0.42	2.67
5		G6	48	4.45	1.19	0.74	2.49
6			16	2.13	0.571	0.36	4.26
7	20.5	G2	800	2.66	0.360	1.00	0.12
8			100	2.03	0.275	0.84	0.38
9			20	1.83	0.248	0.95	0.78
10			4	0.655	0.0887	0.48	1.60
11	42.6		800	5.47	0.360	1.00	0.19
12			100	4.94	0.321	0.98	0.53
13			20	2.3 2	0.151	0.58	1.12
14			4	0.789	0.0515	0.28	2.32

[a]Catalyst activity, in kg active enzyme per cubic meter of beads, used to normalize the rates to force η to unity for tests 1, 2, 7, 11.

[b]Units are kg glucose produced per second per cubic meter of beads.

[c]Units are moles reactant consumer per second per kg active enzyme.

ally. The modulus values thus calculated for each reaction with the three species are listed in the last column of Table 3.

Comparison of Effectiveness Factors to Theory

The effectiveness factors and the moduli given in Table 3 are plotted in the usual manner in Fig. 7. The theoretical first-order curve and the zero-order limit are shown. Michaelis-Menten kinetics ranges from zero order at high concentrations to first order at low concentrations.

The points for maltose and maltotetraose follow the expected behavior well. Previously published results of Swanson (*1*) show similar behavior with maltose for glucoamylase bound to agarose beads. The points for maltohexaose, however, fall somewhat above the expected range, showing a slightly higher rate than would be expected from theory.

The reason for the higher-than-expected reaction rate for maltohexaose may lie in the assumption that the measured glucose production rate was not influenced by successive reactions of the products. The larger molecular weight species, such as maltohexaose, are slower diffusing and faster reacting, and would therefore be more likely to react several times before the products diffused completely out of the bead. This would of course give a higher glucose production rate than that attributable to the maltohexaose reaction alone, resulting in a higher than expected effectiveness factor. Presumably, if the reaction progress were monitored by maltohexaose disappearance rather than glucose production the effectiveness factor would have conformed more closely to the theory. The maltotetraose, being slower reacting and faster diffusing than the maltohexaose, would show this effect to a lesser extent. The maltose data would not be affected at all, since its reaction produces only glucose.

In conclusion, the reaction rates of isolated maltodextrin species in an immobilized glucoamylase catalyst, where pore-diffusion limitations were present, were

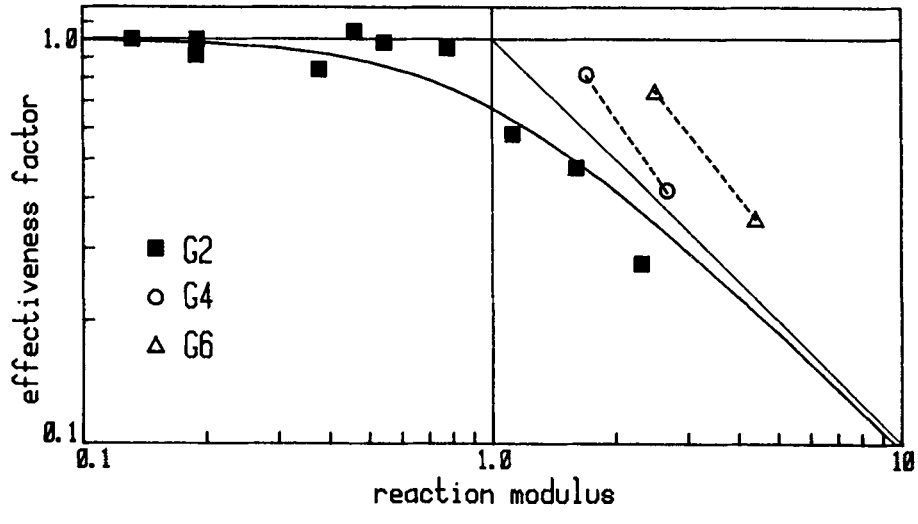

Fig. 7. Effectiveness factor plot for maltose, maltotetraose, and maltohexaose.

predicted by measurements of fundamental physical and chemical properties such as subsite binding affinities and diffusion coefficients. An assumption that the bound enzyme exhibited kinetics different from the soluble enzyme was not needed. The subsite model is especially useful for describing the hydrolysis of the starch components, because the model is mechanistically more fundamental, yet requires fewer parameters than a model based on a series of Michaelis-Menten equations.

References

1. Swanson, S. J., Emery, A., and Lim, H. C. (1978), *AIChE J.* **24,** 30.
2. Lee, D. D., Lee, G. K., Reilly, P. J., and Lee, Y. Y. (1980), *Biotechnol. Bioeng.* **22,** 1.
3. Hiromi, K., Nitta, Y., Numata, C., and Ono, S. (1973), *Biochim. Biophys. Acta* **302,** 362.
4. Swanson, S. J., Emery, A., and Lim, H. C. (1977), *Biotechnol. Bioeng.* **19,** 1715.
5. Miller, G. L., Dean, J., and Blum, R. (1960), *Arch. Biochem. Biophys.* **91,** 21.
6. Somogyi, M. (1945), *J. Biol. Chem.* **160,** 61.
7. Nelson, N. (1944), *J. Biol. Chem.* **153,** 375.
8. Rendina, G., *Experimental Methods in Modern Biochemistry,* Saunders, Philadelphia, 1971.
9. Dahlqvist, A. (1961), *Biochem. J.* **80,** 547.
10. Whelan, W. J., Bailey, J. M., and Roberts, P. J. P. (1953), *J. Chem. Soc.* 1293.
11. French, D., Robyt, J. F., Weintraub, M., and Knock, P. (1966), *J. Chromatogr.* **24,** 68.
12. Ladisch, M. R., Huebner, A. L., and Tsao, G. T. (1978), *J. Chromatogr.* **147,** 185.
13. Brotherton, J. E., Emery, A., and Rodwell, V. W. (1976), *Biotechnol. Bioeng.* **18,** 527.
14. Wang, J. H. (1951), *JACS* **73,** 510, (1952) **74,** 1182; and (with C. V. Robinson, I. S. Edelman), (1953), **75,** 466.
15. Sirotti, D. A., PhD Thesis, Purdue University, 1978.
16. Carslaw, H. C., and Jaeger, J. C. (1959), *Conduction of Heat in Solids,* 2nd ed., Oxford University Press, London.
17. Schneider, P., and Smith, J. M. (1968), *AIChE J.* **14,** 762.
18. Furusawa, T. , Suzuki, M., and Smith, J. M. (1976), *Catal. Rev.* **13,** 43.
19. Lodal, P. N., MSChE Thesis, Purdue University, 1977.
20. Othmer, D. F., and Thakar, M. S. (1953), *Ind. Eng. Chem.* **45,** 589.
21. Bischoff, K. B., *AIChE J.* **11,** 351 (1965).
22. Aris, R., *Ind. Eng. Chem. Fund.* **4,** 227 (1965).
23. Sirotti, D. A., and Emery, A. (1983), *Biotechnol. Bioeng.* **25,** 1773.